XLIII CILAMCE
21-25, November, 2022
FOZ DO IGUAÇU - PR - BRAZIL

The Morley plate element in the frame of a generalized, frequency-dependent hybrid finite element formulation

Renan Costa Sales[1], Ney Augusto Dumont[1]

[1]*Department of Civil and Enviromental Engineering, Pontifical Catholic University of Rio de Janeiro*
Rua Marquês de São Vicente 225, 22451-900, Rio de Janeiro, Brazil
renansales@aluno.puc-rio.br, dumont@puc-rio.br

Abstract. The Morley plate element is the simplest triangular finite element for homogeneous, isotropic material, and represents constant bending curvature/moment exactly, as the flexural counterpart of the membrane, constant strain/stress finite element. It has six degrees of freedom: three corner-node transversal displacements and three edge rotations. We propose a slightly modified, improved Morley element based on a frequency-dependent hybrid finite element formulation to be used in the frame of a generalized modal analysis for stiffness and mass matrices given as frequency power series. The domain stress solution satisfies the homogeneous elastodynamic equilibrium equations for moderately thick plates, as we resort to the concept of mean transversal shear distortion proposed in a previous conference contribution (PANACM/CILAMCE 2021). We show that the formulation for just one mass matrix corresponds to a plain displacement formulation, as proposed in the literature for the thin-plate, static problem (although introducing some due corrections). Some numerical tests with one and two mass matrices show that the model can be seamlessly applied to both moderately-thick and thin plate problems – thus without the shear-locking inconvenience – and in spite of its shape-function simplicity ensures good, asymptotic convergence for natural frequencies. As we have a similar generalized modal development for the membrane triangle, this leads to the simplest – and consistently – conceivable shell element.

Keywords: Morley plate element, Hybrid finite element, Generalized modal analysis

1 Introduction

The dynamic finite element was proposed by Przemieniecki [1] for the frequency-dependent formulation of truss and beam elements. A large number of investigations on this subjected has succeeded, of which we cite just a few [2–7], as a comprehensive account is given by Sales [8].

We propose here a frequency-dependent formulation of the Morley plate element [9], which was originally conceived for the exact static simulation of constant curvature. Our formulation is based on the Hellinger-Reissner potential [10, 11] and makes use of trial functions obtained by solving the homogeneous elastodynamic plate equation to approximate internal bending moments of the triangular plate element [12], for instance.

2 The hybrid stress finite element method

The numerical modelling of time-dependent elastic problems is obtained by means of the Hellinger-Reissner potential, which is based on two fields: a stress field σ^*_{ij} that homogeneously satisfies the equilibrium equations in the domain Ω (fundamental solutions), and a displacement field u^d_i that satisfies the compatibility on the boundary Γ. Whenever such fundamental solutions are available the Hellinger-Reissner potential leads to more accurate results than in the frame of the displacement finite element method.

The time-dependent Hellinger-Reissner variational principle is obtained as a generalization of Hamilton's principle, as presented by Dumont and Oliveira [10]:

$$\begin{aligned}\delta\Pi_{HR} = &\int_{t_0}^{t_1}\int_{\Omega}\left[\left(\sigma^*_{ij,j} + \bar{f}_i - \rho\ddot{u}^*_i\right)\delta u^d_i - \left(\delta\sigma^*_{ij,j} - \rho\delta\ddot{u}^*_i\right)\left(u^*_i - u^d_i\right)\right] d\Omega dt \\ &- \int_{t_0}^{t_1}\int_{\Gamma_\sigma}\left(\sigma^*_{ij}\eta_j - \bar{t}_i\right)\delta u^d_i d\Gamma dt + \int_{t_0}^{t_1}\int_{\Gamma}\delta\sigma^*_{ij}\eta_j\left(u^*_i - u^d_i\right) d\Gamma dt = 0\end{aligned} \tag{1}$$

where u_i^* are displacements associated with the internal stress field σ_{ij}^*, u_i^d are boundary displacements, $\bar{t}_i$ are traction forces, and $\bar{f}_i$ are body forces. Its matrix expression for a given time instant is

$$\delta\mathbf{d}^{\mathrm{T}}\left(-\mathbf{H}^{\mathrm{T}}\mathbf{p}^* - \mathbf{p}^b + \mathbf{p}\right) + \delta\mathbf{p}^{*\mathrm{T}}\left(\mathbf{F}\mathbf{p}^* + \mathbf{b} - \mathbf{H}\mathbf{d}\right) = \mathbf{0} \tag{2}$$

as obtained after representation of σ_{ij}^* and u_i^* in terms of internal force parameters $\mathbf{p}^*$ and interpolation of u_i^d in terms of boundary nodal displacements $\mathbf{d}$. The kinematic matrix $\mathbf{H}$, flexibility matrix $\mathbf{F}$, and equivalent nodal displacement $\mathbf{b}$ and nodal forces $\mathbf{p}$ and $\mathbf{p}^b$ are given as

$$\begin{bmatrix}\mathbf{H} & \mathbf{F} & \mathbf{b}\end{bmatrix} \equiv \int_\Gamma \sigma_{ijm}^*\eta_j \begin{bmatrix}u_{in}^d & u_{in}^* & u_i^b\end{bmatrix} \mathrm{d}\Gamma \tag{3}$$

$$\begin{bmatrix}\mathbf{p} & \mathbf{p}^b\end{bmatrix} \equiv \int_\Gamma \begin{bmatrix}\sigma_{ij}^b\eta_j & \bar{t}_i\end{bmatrix} \mathrm{u}_{in}^d \mathrm{d}\Gamma \tag{4}$$

where n and $m \geq n$ span the sets of boundary nodal displacements $\mathbf{d}$ and internal force parameters $\mathbf{p}^*$, respectively. Solving for $\mathbf{p}^*$ in eq. (2), which holds for arbitrary values of $\delta\mathbf{d}$ and $\delta\mathbf{p}^*$, we obtain the following matrix equilibrium equation, with the subsequent definition of the element's stiffness matrix,

$$\mathbf{K}\mathbf{d} = \mathbf{p} - \mathbf{p}^b + \mathbf{H}^{\mathrm{T}}\mathbf{F}^{-1}\mathbf{b} \quad \Rightarrow \quad \mathbf{K} = \mathbf{H}^{\mathrm{T}}\mathbf{F}^{-1}\mathbf{H} \tag{5}$$

2.1 Frequency-dependent formulation

Assuming that frequency-dependent, fundamental, solutions of σ_{ij}^* and u_i^* exist, as given in the next Section, we expand these solutions as the truncated power series of the frequency ω with $n+1$ terms [3, 7] (here particularly considering that there is no damping)

$$\sigma_{ij}^* = \sum_{k=0}^{n} \omega^{2k} N_{kijm}^* p_m^* \quad , \qquad u_i^* = \sum_{k=0}^{n} \omega^{2k} U_{kim}^* p_m^* \tag{6}$$

with which power series expressions of the nonsingular matrices $\mathbf{F}(\omega)$ and $\mathbf{H}(\omega)$ are also obtained:

$$\mathbf{F}(\omega) = \sum_{k=0}^{n} \omega^{2k}\mathbf{F}_k \quad , \qquad \mathbf{H}(\omega) = \sum_{k=0}^{n} \omega^{2k}\mathbf{H}_k \tag{7}$$

The terms $\mathbf{F}_0$ and $\mathbf{H}_0$ above are the flexibility and kinematic matrices of the elastostatic formulation. Further, we obtain from above the power series expression of the *effective* stiffness matrix $\mathbf{K}$ introduced in eq. (5)

$$\mathbf{K}(\omega) = \mathbf{H}^{\mathrm{T}}(\omega)\mathbf{F}^{-1}(\omega)\mathbf{H}(\omega) = \sum_{k=0}^{n} \omega^{2k}\mathbf{K}_k \equiv \mathbf{K}_0 - \sum_{k=1}^{nN} \omega^{2kn}\mathbf{M}_k \tag{8}$$

where $\mathbf{K}_0$ is the stiffness mass matrix of elastostatic formulation and $\mathbf{M}_k$ are generalized mass matrices. The term $\mathbf{M}_1$ is the consistent mass matrix of the conventional finite element formulation for dynamic problems. Special care must be taken in the evaluation of the inverse of the power series $\mathbf{F}^{-1}(\omega)$, since the first matrix term $\mathbf{F}_0$ in eq. (7) is singular [13]. The particularization to a plate's problem is given in the next Sections.

3 Fundamental solutions for a moderately thick plate

The homogeneous plate governing equation in the frame of the first-order shear deformation theory is

$$K\nabla^4 w^* - \frac{mh^2}{60}\frac{17 - 5\nu}{1 - \nu}\nabla^2\ddot{w}^* + m\ddot{w}^* + \frac{m^2h}{10G}\ddddot{w}^* = 0 \tag{9}$$

where $K = \dfrac{Gh^3}{6(1-\nu)}$ is the plate stiffness, expressed in terms of the Poisson's ratio ν, the shear modulus G and the plate thickness h, and $m = \rho h$ is the mass density per unit area. (See Sales [8], Dumont and Sales [12] for a comprehensive development particularly related to moderately thick plates.) We resort to the potential function

$$\Phi^* = -\left(\nabla^2 + \frac{h^2k^2}{5(1-\nu)}\right) w^* \tag{10}$$

to express the rotations of the plate's reference plane

$$\beta_x^* = \frac{12h^2}{60(1-\nu)-h^4k^2}\left(\frac{5(1-\nu)}{h^2}w^*_{,y} - \Phi^*_{,y}\right), \quad \beta_y^* = \frac{-12h^2}{60(1-\nu)-h^4k^2}\left(\frac{5(1-\nu)}{h^2}w^*_{,x} - \Phi^*_{,x}\right) \tag{11}$$

and write the expression of the bending moments and forces that act on a cross section:

$$\begin{Bmatrix} M^*_{xx} \\ M^*_{yy} \\ M^*_{xy} \end{Bmatrix} = K \begin{bmatrix} 1 & \nu & 0 \\ \nu & 1 & 0 \\ 0 & 0 & \frac{1-\nu}{2} \end{bmatrix} \begin{Bmatrix} \beta^*_{y,x} \\ -\beta^*_{x,y} \\ \beta^*_{y,y} - \beta^*_{x,x} \end{Bmatrix}; \quad \begin{Bmatrix} Q^*_x \\ Q^*_y \end{Bmatrix} = \frac{5Gh}{6} \begin{bmatrix} 1 & 0 \\ 0 & 1 \end{bmatrix} \begin{Bmatrix} \beta^*_y + w^*_{,x} \\ -\beta^*_x + w^*_{,y} \end{Bmatrix} \tag{12}$$

The general frequency-dependent, nonsingular fundamental solution w^* of eq. 9 is expressed in terms of polar coordinates (r, θ) as

$$w^* = (C_{1n} sin(n\theta) + C_{2n}\cos(n\theta))\left(\frac{J_n(k_1 r)}{k_1^n} + \frac{I_n(k_2 r)}{k_2^n}\right)$$
$$+ \frac{C_{3m} sin(m\theta) + C_{4m}\cos(m\theta)}{k_1^2 - k_2^2}\left(\frac{J_m(k_1 r)}{k_1^m} - \frac{I_m(k_2 r)}{k_2^m}\right), \quad n = 0, \ldots, N, \;\; m = n-2 \text{ if } m \geq 0 \tag{13}$$

where $k = \omega\sqrt{\frac{\rho h}{K}}$ is the frequency number and $J_n()$ and $I_n()$ are the Bessel and modified Bessel functions of the first kind and order n. In this equation, n (actually unrelated to the power series numbering of Section 2.1) is the level of complete solution sets deemed necessary in a finite element implementation, with $n = 0$ corresponding to the static solution. Then, we have $1, 2, 3, 4, \ldots, 4$ complete solution sets for each level of $n = 0, 1, 2, 3, \ldots, N$.

The frequency numbers k_1 and k_2 are defined as

$$k_1^2,\; k_2^2 = k\sqrt{1 + k^2\left(\frac{h^2}{120}\frac{7+5\nu}{1-\nu}\right)^2} \pm \frac{k^2h^2}{120}\frac{17-5\nu}{1-\nu} \tag{14}$$

These solutions assume that $k_2^2 \geq 0$, i.e., the maximum plate thickness in this frequency-dependent framework is

$$\frac{17-5\nu}{1-\nu}\frac{h^2 k}{120} \leq 1 \tag{15}$$

Moreover, $k_1 = k_2 = \sqrt{k}$ for the case of thin plates.

4 The frequency-dependent Morley plate element

The Morley plate element has a total of six degrees of freedom: three transversal nodal displacements and three edge rotations, as given in see Fig. 1, where $a_i = x_k - x_j$, $b_i = y_j - y_k$ and $\ell_i = \sqrt{a_i^2 + b_i^2}$, for i, j and k permuting cyclically.

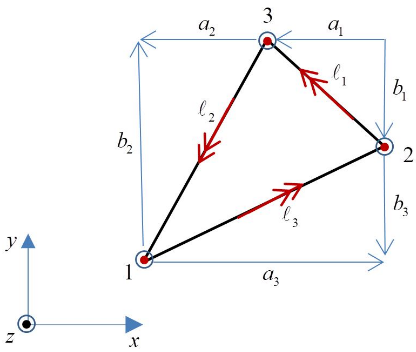

Figure 1. Morley plate element and its Cartesian projections.

The flexibility and kinematic matrices $\mathbf{F} \equiv \mathbf{F}(\omega)$ and $\mathbf{H} \equiv \mathbf{H}(\omega)$ of eq. (7) are expressed for the frequency-dependent hybrid Morley plate element (here called HMPT6) in matrix format as

$$\begin{bmatrix} \mathbf{H} & \mathbf{F} \end{bmatrix} = \int_\Gamma \mathbf{N}^{*\mathrm{T}}\mathbf{T}^{\mathrm{T}} \begin{bmatrix} \mathbf{U} & \mathbf{U}^* \end{bmatrix} \mathrm{d}\Gamma \tag{16}$$

$$\mathbf{N}^* = \begin{bmatrix} M^*_{mxx} & M^*_{myy} & M^*_{mxy} & Q^*_{mx} & Q^*_{my} \end{bmatrix}^{\mathrm{T}}, \quad \begin{bmatrix} \mathbf{U}^* \\ \mathbf{U} \end{bmatrix} = \begin{bmatrix} \beta^*_{my} & \beta^*_{mx} & w^*_m \\ \beta^d_{ny} & \beta^d_{ny} & w^d_n \end{bmatrix}^{\mathrm{T}} \tag{17}$$

with the terms affected by the subscripts $m = 1, \ldots, 6$ and $n = 1, 2, 3$ related to the fundamental solutions and boundary interpolation functions, respectively, according to the general eq. (3) and particularized for the plate eq. (12). As indicated in eq. (7), $\mathbf{N}^*$ and $\mathbf{U}^*$ are actually to be expressed in terms of power series expansions which demands a tedious manipulation [8]. We also have in eq. (16) the matrix of unit normal projections

$$\mathbf{T} = \begin{bmatrix} \eta_x & 0 & \eta_y & 0 & 0 \\ 0 & -\eta_y & -\eta_x & 0 & 0 \\ 0 & 0 & 0 & \eta_x & \eta_y \end{bmatrix} \tag{18}$$

Using in eq. (13) $N = 3$ we obtain a total of six internal solutions, the dimension of vector $\mathbf{p}^*$ in eq. (2), which is then exactly the dimension of vector $\mathbf{d}$, Morley triangle's degrees of freedom. This is also a complete set of solutions, which assures that no spurious modes are likely to rise in the computational course.

By the way, The 3×3 flexibility matrix $\mathbf{F}_0$, thus for $n = 2$ and $\omega \to 0$ in eq. (13) and eliminating the rigid-body terms to only correspond to the static case, turns out to be simply

$$\mathbf{F}_0 = \frac{16A}{K} \begin{bmatrix} 1-\nu & 0 & 0 \\ 0 & 1-\nu & 0 \\ 0 & 0 & 1+\nu \end{bmatrix} \tag{19}$$

where A is the triangle's area. The corresponding 3×6 kinematic matrix $\mathbf{H}_0$ also becomes expressible analytically:

$$\mathbf{H}_0 = 4(1-\nu) \begin{bmatrix} \dfrac{2A(a_2b_3 + a_3b_2)}{\ell_3^2\ell_2^2} & \dfrac{2A(b_3b_2 - a_2a_3)}{\ell_3^2\ell_2^2} & 0 \\ \dfrac{2A(a_1b_3 + a_3b_1)}{\ell_3^2\ell_1^2} & \dfrac{2A(b_3b_1 - a_1a_3)}{\ell_3^2\ell_1^2} & 0 \\ \dfrac{2A(a_1b_2 + a_2b_1)}{\ell_1^2\ell_2^2} & \dfrac{2A(b_1b_2 - a_1a_2)}{\ell_1^2\ell_2^2} & 0 \\ -\dfrac{a_3b_3}{\ell_3} & \dfrac{a_3^2 - b_3^2}{2\ell_3} & -\dfrac{\ell_3}{2}\left(\dfrac{1+\nu}{1-\nu}\right) \\ -\dfrac{a_1b_1}{\ell_1} & \dfrac{a_1^2 - b_1^2}{2\ell_1} & -\dfrac{\ell_1}{2}\left(\dfrac{1+\nu}{1-\nu}\right) \\ -\dfrac{a_2b_2}{\ell_2} & \dfrac{a_2^2 - b_2^2}{2\ell_2} & -\dfrac{\ell_2}{2}\left(\dfrac{1+\nu}{1-\nu}\right) \end{bmatrix}^{\mathrm{T}} \tag{20}$$

The expressions of $\mathbf{F}_0$ and $\mathbf{H}_0$ above lead according to eq. (5) to the same result of the displacement finite element, as proposed by Morley.

On the other hand, the consistent mass matrix $\mathbf{M}_1$ obtained according to eq. (16) turns out to be not positive definite, in general. The reason for that seems to be the fact that some important contribution is smeared out in the expression of the expansion terms of $\mathbf{H}_1$ related to the edge rotations. (Maybe we are just overseeing some problem-related geometric interpretation.)

As a way to overcome this, we decided to evaluate $\mathbf{H}$ in terms of domain integrations by directly using the quadratic interpolation functions proposed by Morley [9]. As a matter of fact, Abdalla and Hassan [15] presented a simple way to express these domain shape functions in terms of eccentricity coefficients $e_i = (\ell_k^2 - \ell_j^2)/\ell_i^2$, which are, after fixing some printing errors of the original contribution,

$$\begin{bmatrix} N_1 \\ N_2 \\ N_3 \\ N_4 \\ N_5 \\ N_6 \end{bmatrix} = \begin{bmatrix} 1 & 0 & 0 & {}^1\!/_2\,(1+e_2) & {}^1\!/_2\,(2+e_2-e_3) & {}^1\!/_2\,(1-e_3) \\ 0 & 1 & 0 & {}^1\!/_2\,(1-e_1) & {}^1\!/_2\,(1+e_3) & {}^1\!/_2\,(2+e_3-e_1) \\ 0 & 0 & 1 & {}^1\!/_2\,(2+e_1-e_2) & {}^1\!/_2\,(1-e_2) & {}^1\!/_2\,(1+e_1) \\ 0 & 0 & 0 & 0 & 2A/\ell_3 & 2A/\ell_3 \\ 0 & 0 & 0 & 2A/\ell_1 & 0 & 2A/\ell_1 \\ 0 & 0 & 0 & 2A/\ell_2 & 2A/\ell_2 & 0 \end{bmatrix} \begin{Bmatrix} \xi_1^2 \\ \xi_2^2 \\ \xi_3^2 \\ \xi_1\xi_2 \\ \xi_2\xi_3 \\ \xi_3\xi_1 \end{Bmatrix} \tag{21}$$

Then, it is a simple matter to transform the boundary integral expression of $\mathbf{H}$ in eq. (16) into a domain one as well to obtain the domain expression of the displacement interpolation functions we have just introduced.

5 Numerical tests

5.1 Simply supported square plate subjected to static, uniform load

In this example we just test the Morley plate element implemented in the frame of our HMPT6 model. The hybrid triangular elements HMPT6 is employed to solve the problem of a square plate under uniform load $q = 1$. The simply supported square plate has edges $L = 10$, thickness $h = 1$ and is subjected to uniform load $q = 1$, in consistent units. Elastic modulus and Poisson's ratio are $E = 10.92$ and $\nu = 0.30$. Table 1 shows the results of central displacement and central bending moment of the plate for several mesh discretizations, which are actually symmetric about four planes. Although we have not taken advantage of these symmetries in the numerical implementations, it is worth noticing that the very coarse 2×2 mesh would actually require the use of only one triangle element and one degree of freedom. The bending moments at the plate middle are given as the average of the constant values measured on the adjacent elements. The target solutions are given by Timoshenko and Woinowsky-Krieger [16].

5.2 Free vibration of a simply supported square plate

In this example, the plate has edges $L = 10m$ and thickness $h = 0.01m$. The material properties are $E = 200GPa$, $\nu = 0.30$ and mass density $\rho = 8000Kg/m^3$. The associated, generalized nonlinear eigenvalue problem is solved by means of the modified Jacobi-Davidson algorithm developed by Dumont [7].

Table 2 shows the results of the first five normalized natural frequencies $\bar{\omega} = \left(\frac{\omega^4 \rho L^4 h}{K}\right)^{1/4}$ for the element HPMT6 with one (1MM) and two (2MM) mass matrices. We observe good convergence for both results HMPT6-1MM and HMPT6-2MM. Nevertheless, the second mass matrix does not seem to improve the computed natural frequency values, which differs from the results observed for frequency-dependent membrane elements [8]. As expected, the contribution of a second mass matrix becomes less perceptible as mesh refinement increases. A second mass matrix leads to smaller frequency values, which is also expected. On the other hand, convergence with mesh refinement occurs from inferior values, which makes the contribution of a second mass matrix a contradiction, at least for the present example.

5.3 Free vibration of a rhombic plate

We simulate the free vibration of a rhombic plate with skew angle 60^0 and ratio $L/h = 5$. The plate is clamped on one border and free on the other borders (CFFF). The material properties are $E = 200GPa$, $\nu = 0.30$ and $\rho = 8000Kg/m^3$.

Table 3 shows the first five normalized natural frequencies, evaluated according to our computer implementation, as compared with results by Karunasena et al. [17].This is in principle a more challenger problem than in the previous example, as there are no symmetries. However, the same conclusions drawn above apply unchanged to this case.

Table 1. Results of central displacements and bending moments for the uniformly loaded, simply supported plate.

Mesh	DOF	$w_c/(qL^4/100K)$	$M_c/(qL^4/100)$
2×2	25	0.71857	4.30936
4×4	81	0.48866	4.62130
8×8	289	0.42729	4.74006
16×16	1089	0.41153	4.77594
Reference solution[16]		0.4062	4.7890

Table 2. First five natural frequencies of a simply supported square plate using plate hybrid elements.

Element	Mesh	Mode 1	Mode 2	Mode 3	Mode 4	Mode 5
HMPT6-1MM	4×4	4.16572	6.08796	6.16202	7.64991	7.81313
	8×8	4.35650	6.66892	6.69717	8.33015	9.03759
	16×16	4.41982	6.74163	6.74964	8.48615	9.39471
HMPT6-2MM	4×4	4.16508	5.75764	5.82768	7.35590	7.77771
	8×8	4.35645	6.30708	6.33379	7.87817	8.54723
	16×16	4.41982	6.74163	6.74964	8.48615	9.39471
Analytical solution		4.44288	7.02481	7.02481	8.88577	9.93459

Table 3. First five natural frequencies of a rhombic plate (CFFF) with ratio $L/h = 5$.

Element	Mesh	Mode 1	Mode 2	Mode 3	Mode 4	Mode 5
HMPT6-1MM	2×2	0.2616	0.7658	0.8661	1.3789	1.5545
	4×4	0.3325	0.7542	1.4000	1.8364	2.4995
	8×8	0.3717	0.8276	1.9261	2.2753	3.0551
HMPT6-2MM	2×2	0.2614	0.7624	0.8610	1.3663	1.5261
	4×4	0.3154	0.7542	1.3954	1.8364	2.3728
	8×8	0.3717	0.7852	1.9200	2.2630	3.0641
Reference solution [17]		0.3770	0.8170	1.9810	2.1660	3.1040

6 Conclusions

We proposed a more general approach of the Morley plate element, which is based on a hybrid frequency-dependent plate formulation that satisfies the homogeneous elastodynamic plate governing equations.

The eigenfrequency evaluations with the implemented element showed good convergence, although we do not observe better results by applying two mass matrices. We are presently carrying out investigations for the time response in terms of modal analysis. This would elucidate whether or not additional mass matrices contribute to better results for plate elements, as this is definitely the case for beam and membrane elements.

Acknowledgements. This project was supported by the Brazilian agencies CAPES and CNPq.

Authorship statement. The authors hereby confirm that they are the sole liable persons responsible for the authorship of this work, and that all material of the present paper is the property (and authorship) of the authors.

References

[1] J. S. Przemieniecki. *Theory of matrix structural analysis*. McGraw-Hill, New York, 1968.

[2] M. Paz and L. Dung. Power Series Expansion of the Error Function. *International Journal for Numerical Methods in Engineering*, vol. 9, pp. 449–459, 1975.

[3] N. A. Dumont and R. De Oliveira. From frequency-dependent mass and stiffness matrices to the dynamic response of elastic systems. *International Journal of Solids and Structures*, vol. 38, pp. 1813–1830, 2001.

[4] K. K. Gupta. Development of a finite dynamic element for free vibration analysis of two-dimensional structures. *International Journal for Numerical Methods in Engineering*, vol. 12, n. 8, pp. 1311–1327, 1978.

[5] G. He, D. Chen, and T. H. Pian. Finite dynamic element formulation for three-dimensional structures. *Communications in Numerical Methods in Engineering*, vol. 16, n. 5, pp. 357–362, 2000.

[6] N. A. Dumont and A. C. De Oliveira. A dynamic interaction model of railway track structural elements. In *Proceedings of the XXVII Ibero-Latin-American Congress on Computational Methods in Engineering*, pp. 16 on CD, Belém, Brazil, 2006.

[7] N. A. Dumont. On the solution of generalized non-linear complex-symmetric eigenvalue problems. *International Journal for Numerical Methods in Engineering*, vol. 71, n. 13, pp. 1534–1568, 2007.

[8] R. C. Sales. *Implementation of frequency-dependent hybrid finite elements for the analysis of thin or moderately thick plates and shells*. PhD thesis, Pontifical Catholic University of Rio de Janeiro. (In progress), 2022.

[9] L. S. Morley. The constant-moment plate-bending element. *The Journal of Strain Analysis for Engineering Design*, vol. 6, n. 1, pp. 20–24, 1971.

[10] N. A. Dumont and P. G. C. Prazeres. Hybrid dynamic finite element families for the general analysis of the time-dependent problems. In *Procs. ICSSD 2005 - Third International Conference on Structural Stability and Dynamics*, pp. 10 in CD, Florida (EUA), 2005.

[11] N. A. Dumont and C. A. Aguilar Marón. Linear algebra issues in a family of advanced hybrid finite elements. *Computational Methods in Applied Sciences*, vol. 24, pp. 255–275, 2011.

[12] N. A. Dumont and R. C. Sales. Consistency assessment of plate bending theories for the implementation of efficient hybrid finite elements in linear statics and dynamics. In *Proceedings of the XLII Ibero-Latin-American Congress on Computational Methods in Engineering and III Pan-American Congress on Computational Mechanics*, pp. 7, Rio de Janeiro, Brazil, 2021.

[13] N. A. Dumont. On the inverse of generalized λ-matrices with singular leading term. *International Journal for Numerical Methods in Engineering*, vol. 66, n. 4, pp. 571–603, 2006.

[14] J. B. Huang, S. Cen, Y. Shang, and C. F. Li. A new triangular hybrid displacement function element for static and free vibration analyses of Mindlin-Reissner plate. *Latin American Journal of Solids and Structures*, vol. 14, n. 5, pp. 765–804, 2017.

[15] H. Abdalla and K. Hassan. Shape effect on Morley's element. *Communications in Numerical Methods in Engineering*, vol. 1, n. 5, pp. 255–259, 1985.

[16] S. Timoshenko and S. Woinowsky-Krieger. *Theory of plate and shells*. McGraw-Hill, New York, 2nd edition, 1959.

[17] W. Karunasena, K. M. Liew, and F. G. Al-Bermani. Natural frequencies of thick arbitrary quadrilateral plates using the pb-2 Ritz method. *Journal of Sound and Vibration*, vol. 196, n. 4, pp. 371–385, 1996.